

Final Report for the ISEE/ICE Guest Investigator Proposal Entitled
"Broadband Electrostatic Noise and Ion Beam Dynamics in the Magnetotail"

There are two main areas which we have emphasized our effort towards the understanding of the mechanism responsible for the broadband electrostatic noise (BEN) observed in the magnetotail. The first area concerns our work on the generation of BEN in the boundary layer region of the magnetotail whereas the second area concerns the occasional presence of BEN in the neutral sheet region.

For the generation of BEN in the boundary layer region, we have developed the hybrid simulation code to the point where we can reliably perform longtime, quiet, highly resolved simulations of field aligned electron and ion beam flow. The result of the simulation shows that broadband emissions cannot be generated by beam-plasma instability if realistic values of the ion beam parameters are used. The waves generated from beam-plasma instability are highly discrete and are of high frequencies. For the plasma sheet boundary layer condition, the wave frequencies are in the kHz range, which is incompatible with the observation that the peak power in BEN occur in the 10's of Hz range. We find that the BEN characteristics are more consistent with lower hybrid drift instability as first discussed by Huba et al (1977) and later on supported observationally by Cattell and Mozer (1987).

For the occasional presence of BEN in the neutral sheet region, we have performed a linear analysis of the kinetic cross-field streaming instability appropriate to the neutral sheet condition just prior to onset of substorm expansion. By solving numerically the dispersion relation, we find that the instability has a growth time comparable to the onset time scale of substorm onset. The excited waves have a mixed polarization in the lower hybrid frequency range. The imposed drift driving the instability corresponds to unmagnetized ions undergoing current sheet acceleration in the presence of a cross-tail electric field. The required electric field strength is in the 10 mV/m range which is well within the observed electric field values detected in the neutral sheet during substorms. This finding can potentially account for the disruption of cross-tail current and its diversion to the ionosphere to form the substorm current wedge. Furthermore, a number of features associated with substorm expansion onset can be understood based on this substorm onset scenario (see enclosed preprint).

(NASA-CR-186260) A CURRENT DISRUPTION
MECHANISM IN THE NEUTRAL SHEET FOR
TRIGGERING SUBSTORM EXPANSIONS Final Report
(JHU) 23 p

CSCCL 03B

N90-17525

Unclass

6/90 0257082

A Current Disruption Mechanism in the Neutral Sheet
For Triggering Substorm Expansions

by

A. T. Y. Lui

Applied Physics Laboratory, Johns Hopkins University
Laurel, Maryland 20707

A. Mankofsky, C.-L. Chang, K. Papadopoulos
Science Applications International Corporation,
McLean, Virginia 22102

and

C. S. Wu

Institute for Physical Science and Technology,
University of Maryland, College Park, Maryland 20742

Submitted to Geophysical Research Letters

Revised, December, 1989

ABSTRACT

A linear analysis is performed to investigate the kinetic cross-field streaming instability in the Earth's magnetotail neutral sheet region. Numerical solution of the dispersion equation shows that the instability can occur under conditions expected for the neutral sheet just prior to the onset of substorm expansion. The instability results in the excitation of whistler waves with a mixed polarization in the lower hybrid frequency range propagating obliquely to the local magnetic field. The ensuing turbulence of this instability can lead to a reduction of the cross-tail current which drives the instability, causing the current to continue through the ionosphere with the formation of a substorm current wedge. A substorm expansion onset scenario is proposed based on this instability in which the relative drift between ions and electrons is primarily due to unmagnetized ions undergoing current sheet acceleration in the presence of a cross-tail electric field. The required electric field strength is within the range of electric field values detected in the neutral sheet region during substorm intervals. The skew in local time of substorm onset location and the three conditions under which substorm onset is observed can be understood on the basis of the proposed scenario.

INTRODUCTION

The initiation of the expansion phase of a magnetospheric substorm is generally considered to involve a process by which the near-earth portion of the cross-tail current in the magnetotail is drastically reduced or disrupted. The current disruption is accompanied by a diversion of the cross-tail current into the ionosphere, forming a current wedge. The radial extent of current disruption has been estimated quantitatively for a small substorm to be $\sim 3.5 R_E$ in the innermost portion of the current sheet [Lui, 1978].

In many theoretical models, the substorm onset is attributed to plasma instabilities in the neutral sheet. The tearing instability has been discussed extensively in the literature as one possible candidate [e.g. Galeev, 1979; see also Coroniti, 1985 for a critique]. Since cross-field currents exist in the magnetotail, it is natural to consider cross-field current-driven instabilities. Huba et al [1978] have proposed that the lower hybrid drift instability (LHDI) due to a diamagnetic current may account for the broadband electrostatic noise present in the high latitude boundary of the plasma sheet. This instability has been explored further in terms of its penetration to the neutral sheet, but with little success [Huba and Papadopoulos, 1978]. The mode is stabilized rapidly by the increasing plasma beta and the decreasing density gradient as the neutral sheet is approached.

Another instability of interest is the kinetic cross-field streaming instability (KCSI) first discussed by Wu et al. [1983]. The KCSI has been suggested to explain microturbulence and plasma heating in collisionless shock waves [Wu et al., 1984; Winske et al., 1985]. The purpose of this paper is to suggest that both KCSI and LHDI play important roles in triggering substorms, with the former operating in the neutral sheet and the latter in the higher

latitude plasma sheet. Numerical results of KCSI calculation are shown to demonstrate its importance in the Earth's neutral sheet. Implications based on this scenario for substorm expansion onset are then discussed.

SCENARIO FOR SUBSTORM EXPANSION ONSET

There are several observed features in the magnetotail leading up to substorm expansion (see, e.g. Akasofu, 1977). Prior to the expansion phase onset, the magnetic field configuration in the near-earth plasma sheet is noted to become very tail-like, implying that the cross-tail current intensifies tremendously [Kaufmann, 1987]. The magnetic field lines are stretched out further down the tail and the plasma sheet is thinned to the extent that the ions become unmagnetized in the neutral sheet region when their gyroradii are larger than the field gradient scale length. Kaufmann has noted that an integrated current density of 300 mA/m is required to create tail-like field configuration near the geosynchronous altitude. If the near-earth plasma sheet is thinned to $0.5 R_E$ at this time, then the average current density is $0.1 \mu\text{A}/\text{m}^2$. For a number density of 0.3 cm^{-3} , the relative drift between electrons and ions is 2000 km/s. If the magnetic field is taken to be 5 nT, this relative drift corresponds to $\sim 10 v_A$, which will give rise to a significant growth of the KCSI as will be shown later (Figure 2).

We suggest that current disruption in the tail at substorm expansion onset is due to the combined effect of the KCSI in the neutral sheet and the LHDI outside the neutral sheet. Figure 1 illustrates this idea and the coordinate system used in the KCSI calculation. The cross-field drift for the KCSI arises from ions becoming unmagnetized in the neutral sheet (executing Speiser [1965] orbits) and undergoing acceleration in a cross-tail electric

field. On the other hand, the free energy source for the LHDI comes from the diamagnetic current associated with a density gradient which is increased considerably by plasma sheet thinning prior to substorm onset. Since the LHDI has already been discussed extensively [Huba et al., 1977, 1981], we shall focus on the KCSI in the neutral sheet region.

KINETIC CROSS-FIELD STREAMING INSTABILITY FOR SUBSTORM ONSET

The dispersion equation under consideration is basically the same as that given by Wu et al. [1983]. The appendix provides the details of this dispersion equation. It is useful to consider some approximate properties of the instability before discussing the numerical results. Following the approach used in Wu et al [1983], one can show that when the ion beta β_i is large, the growth rate γ of the unstable mode can be expressed as

$$\gamma/\omega_r = -\pi^{1/2} \sin^2\theta [\xi_i/\beta_i + 0.5 \beta_e \xi_e \exp(-\xi_e^2)] \quad (1)$$

where $\theta = \cos^{-1}(\hat{k} \cdot \hat{B})$ and ω_r is the real frequency given by the approximate whistler dispersion relation $\omega_r \approx k^2 c^2 \cos \theta / \omega_{pe}^2$. The other parameters are defined in the appendix, e.g., ξ_i and ξ_e are given in Eq. (A8). Several basic features are indicated in Eq. (1). First, the growth rate diminishes as θ approaches zero. Second, the KCSI can set in when the drift speed v_o is sufficiently large such that the electron Landau damping is overcome by the ion contribution to growth. Third, the growth rate decreases when the ion beta increases.

We have solved Eq. (A3) numerically with a dispersion solver which has been benchmarked by solutions given in Wu et al. [1983]. For our study,

we adopt $n_e = n_i = 0.3 \text{ cm}^{-3}$, $T_i/T_e = 10$, $T_i = 2 \text{ keV}$, and $B_z = 5 \text{ nT}$ for the neutral sheet [Huang et al., 1989]. These parameters give a plasma beta $\beta_i \approx 10$, $\omega_{pe}/\Omega_e \approx 35$ and the Alfvén speed $v_A \approx 200 \text{ km/s}$. Note that previous studies of this instability dealt with plasma regimes with $\beta \lesssim 1$. The plasma beta in our situation is about an order of magnitude higher.

Figure 2a shows the wave frequency and growth rate maximized over both the normalized wavenumber kp_e and the propagation angle θ for drift speeds ranging from about $2.5 v_A$ to $20 v_A$. The normalization for ω and γ is the lower hybrid frequency $\omega_{lh} = \omega_{pi}/(1 + \omega_{pe}^2/\Omega_e^2)^{1/2}$, which is about 20 rad/s in our case. A significant growth rate for the KCSI is found at drift speed just below $2.5 v_A$. Both the frequency and the growth rate become larger with increasing drift speed. At $v_o/v_A = 5, 10, 20$, we find $\omega/\omega_{lh} \approx 0.13, 0.42, 1.26$ and $\gamma/\omega_{lh} \approx 0.0072, 0.032, 0.104$ (corresponding to an e-folding time of about 43 s, 9 s, 3s), respectively. The growth rates should be considered as lower limits since Chang and Wong [1989] have recently shown that the inclusion of electromagnetic response of ions in high β regime can enhance considerably the growth rate. The excited waves have comparatively long wavelength ($kp_e \approx 0.06$ to 0.2) and small propagation angle ($\theta \approx 33^\circ$ to 55°). The occurrence of growth for obliquely propagating waves at $v_o \gg v_A$ has been demonstrated by Wu et al. [1983] although it is contrary to the simple intuitive feeling on the effects of Landau damping in oblique waves.

The nature of waves excited due to the KCSI has been examined carefully by Wu et al. [1983] who have determined them to be whistlers. The ratio of electromagnetic to electrostatic components, plotted in Figure 2b, shows that the two components are comparable at low drift speeds. However, the electromagnetic component becomes more dominant as the drift speed increases. Ion heating is expected since the free energy driving this

instability comes from the ion drift. Electron heating is also anticipated as ξ_e is small ($\lesssim 0.1$). Substantial growth is found over a broad range of θ (10° to 50°), as illustrated in Fig. 3.

IMPLICATIONS FROM THIS SUBSTORM ONSET SCENARIO

If the initiation of substorm expansion is due to the onset of KCSI in the neutral sheet and LHDI outside the neutral sheet, then there are several implications which compare favorably with our present knowledge on the conditions under which substorm onset occurs. The instability growth in the neutral sheet depends critically on the relative drift between the ions and electrons. One possible way to enhance the relative drift is the cross-tail electric field. Since the ions are unmagnetized in the neutral sheet just prior to the substorm expansion onset, they undergo Speiser orbits and can be accelerated in the direction of the cross-tail electric field.

Under the above scenario, several observed features connected with substorm expansion onset can be accounted for by the proposed mechanism. The local time of substorm onset is known to be typically skewed towards the evening sector [e.g., Craven and Frank, 1989]. If the cross-tail electric field is the primary agent for increasing the relative drift, then it is natural to expect the highest speed attained by the unmagnetized ions to occur at the evening side of the thinned current sheet region in the midnight sector, perhaps even with ions making multiple neutral sheet encounters. Thus, the substorm onset is typically skewed towards the evening sector.

There are three conditions identified observationally which can trigger a substorm onset (see, e.g. Baumjohann, 1986), namely, (1) by northward turnings of the interplanetary magnetic field (IMF) during a

southward IMF period, (2) by sudden enhancement of solar wind pressure, and (3) by an apparently internal process during steady southward IMF (with no identifiable onset signature in the solar wind). Substorms initiated by the first two conditions can be considered as being directly driven whereas those initiated by the third condition are due to unloading.

The first condition, suggested first by Rostoker [1983], can be understood in the following manner. During southward IMF, the auroral ovals expand, indicating an increase in the total magnetic flux content of the tail lobes. Assuming the tail lobe to be cylindrically symmetric, this increase in tail flux implies an induced electric field pointing dusk-to-dawn in the current sheet of the magnetotail, thus reducing the cross-tail dawn-to-dusk electric field generated by the solar wind-magnetosphere dynamo (D. G. Mitchell and G. Rostoker have independently arrived at the same idea). Therefore, northward turning of IMF at this time will decrease the opposing induced electric field, resulting in a sudden increase in the electric field in the dawn-to-dusk direction, which will in turn lead to an enhanced current sheet acceleration of ions in the neutral sheet to initiate the KCSI.

For the second triggering condition, it is observed that sudden solar wind pressure enhancement leads to compression and thinning of the plasma sheet. This is presumably accompanied by an enhanced dawn-to-dusk electric field which convects magnetotail plasma into the neutral sheet region, building up pressure in response to the larger external pressure. Again, the thinned plasma sheet leads to ions being unmagnetized in the neutral sheet and the enhanced electric field will increase the ion drift to drive the KCSI.

Finally, for the third triggering condition, it is well recognized from observations that both the cross-tail electric field and the B_z component in the neutral sheet (the two quantities that determine the amount of ion

acceleration in the current sheet region) often exhibit large variations [Cattell and Mozer, 1987]. During southward IMF, it is very likely that these variations in localized regions of the current sheet can elevate the ion drift speed high enough to yield a favorable condition for the onset of the KCSI.

One can estimate the electric field strength required to trigger the proposed instability in the current sheet. The approximate energy gained from current sheet acceleration can be obtained by considering an ion executing a Speiser orbit and drifting in the direction of the electric field through a distance equal to twice its gyroradius. For a 2 keV ion, the gyroradius in an ambient magnetic field of 5 nT is about 1300 km. A relative drift speed of 1000 km/s ($\approx 5 v_A$) requires an acceleration of only 3.2 keV, corresponding to an averaged electric field strength of ~ 1 mV/m. A drift speed of 2000 km/s ($\approx 10 v_A$) requires an acceleration of 19 keV and an averaged electric field of ~ 7 mV/m. Electric fields of this strength and higher have been reported in the current sheet region during substorms [Cattell and Mozer, 1987]. Furthermore, the waves in the vicinity of the neutral sheet detected during substorms are found to have peak power at frequencies near the lower hybrid frequency as predicted by the instability analysis performed here.

Although the magnitude of current reduction by this instability has not been determined by non-linear analysis yet, we speculate here the plausible consequences. The current disruption mechanism can lead to collapse of highly stretched field lines into more dipolar field lines, resulting in plasma sheet thickening. This change in magnetic field configuration, known as dipolarization, will also energize the particles via Fermi acceleration (shortening of field lines) and betatron acceleration (field magnitude increase as a result of the collapse). The turbulence due to LHDI outside the neutral sheet reduces the diamagnetic current (which is the energy source for

LHDI) and therefore decreases the density gradient scale length. This leads to thickening of the plasma sheet, augmenting the thickening arising from dipolarization. Observations indeed show plasma sheet thickening associated with dipolarization.

DISCUSSION AND CONCLUSIONS

We have obtained numerical solutions to the linear dispersion equation of the kinetic cross-field streaming instability in the Earth's magnetotail neutral sheet environment. The result demonstrates that this instability can have a growth time comparable to the substorm onset time. The most probable onset location in the tail is where the strongest current flows, i.e. where the magnetic field configuration changes from dipolar to tail-like, as suggested earlier by Lui and Burrows [1978]. Since this is a cross-field current-driven instability, its growth will lead to a local current reduction, which forces part of the cross-tail current to continue through the ionosphere due to the large inductance of the current system. A current wedge is thus formed. However, if the ionospheric condition is not appropriate for the imposed current (see, e.g., the treatment by Kan et al., 1988), then the current diversion is impeded by the modification of magnetospheric electric fields through Alfvén waves bouncing between the two regions. A pseudo-breakup phenomenon may result instead.

The excited waves resulting from the instability have a mixed polarization with comparable electromagnetic and electrostatic components. Enhanced magnetic turbulence in the neutral sheet is therefore anticipated, consistent with in situ observations of current disruption [Lui et al., 1988]. The wave frequencies are in the lower hybrid frequency range, in agreement

with observations also [Cattell and Mozer, 1987]. Heating is expected for both ions and electrons. The current disruption region may be perceived as a 3-D turbulent reconnection region with a dynamo process as envisioned by Song and Lysak [1989] in the dayside magnetopause. The current disruption mechanism causes dipolarization which can energize particles further via Fermi and betatron acceleration.

The cross-tail electric field plays an important role in enhancing the relative drift between ions and electrons to drive the instability. Note that dipolarization is associated with an induced dawn-to-dusk electric field which will accelerate unmagnetized ions in adjacent regions and will lead to further spatial spreading of the unstable region in the neutral sheet. This corresponds to the local time widening of the substorm current wedge and radial spreading of the disturbance. The electric field magnitude needed to initiate the instability is within the range of electric fields often observed in the neutral sheet during substorm periods.

The scenario developed for substorm expansion onset based on this mechanism can readily account for the observed fact that the local time for substorm onset is typically skewed towards the evening sector from the midnight meridian. Furthermore, the three conditions in the solar wind under which substorm onset is observed can be understood.

APPENDIX

We outline here the dispersion equation used in our calculation. For specie α ($\alpha = i$ or e), $T_\alpha = \frac{1}{2} m_\alpha v_\alpha^2$ is the temperature, m_α is the mass, v_α is the thermal speed, $\Omega_\alpha = |e|B/m_\alpha$ is the gyrofrequency, $\rho_\alpha = v_\alpha/\Omega_\alpha$ is the gyroradius, n_α is the number density, β_α is the plasma beta, and $\omega_{p\alpha}$ is the

plasma frequency. The waves under consideration here have frequencies between Ω_i and Ω_e ($\Omega_i \ll \omega \ll \Omega_e$) and wavelengths much smaller than the ion gyroradius ρ_i ($k\rho_i \gg 1$). Therefore, it is reasonable to take electrons to be magnetized while ions are taken to be unmagnetized. In fact, this condition is also suggested by observations for the neutral sheet region just prior to substorm expansion onset. The local equilibrium distribution functions for electrons and ions are, respectively,

$$F_e = n_e (\pi v_e^2)^{-3/2} \exp(-v^2/v_e^2), \quad (\text{A1})$$

$$F_i = n_i (\pi v_i^2)^{-3/2} \exp\{-[v_x^2 + (v_y - v_o)^2 + v_z^2]/v_i^2\}, \quad (\text{A2})$$

where v_o is the ion drift velocity perpendicular to the ambient magnetic field. The above forms indicate that our analysis will be performed in the guiding center rest frame of the electrons using the coordinate system given in Figure 1. Taking the local approximation, neglecting the higher harmonic terms in the electron orbit integration, and considering waves propagating in the yz-plane, i.e., $\vec{k} = k_{\parallel} \frac{\vec{B}}{B} + k_y \hat{e}_y$, we find the dispersion equation to be

$$1 + \chi_i(\omega, k) + \chi_{e,1}(\omega, k) + \chi_{e,2}(\omega, k) = 0. \quad (\text{A3})$$

The first term in Eq. (A3) is the displacement current contribution, the second and third terms are electrostatic contributions from the ions and the electrons, respectively, and the last term contains the electromagnetic effects. The terms are explicitly given as

$$\chi_i(\omega, k) = \frac{2 \omega_{pi}^2}{k^2 v_i^2} [1 + \xi_i Z(\xi_i)], \quad (\text{A4})$$

$$\chi_{e,1}(\omega, k) = \frac{2 \omega_{pe}^2}{k^2 v_e^2} (1 - \phi_3), \quad (A5)$$

$$\chi_{e,2}(\omega, k) = \frac{4 \omega_{pe}^4}{k^4 c^2 v_e^2} \frac{D_1 + D_2 + D_3 + D_4}{D_5 + D_6}, \quad (A6)$$

where $D_1 = -\frac{4\omega_{pe}^2}{k^2 c^2} \phi_2 \phi_4 \phi_5$, $D_2 = \phi_4^2 \left[1 - \frac{\omega^2}{k^2 c^2} + \frac{2 \omega_{pe}^2}{k^2 c^2} \phi_1 \right]$,

$$D_3 = \phi_2^2 \left[1 - \frac{\omega^2}{k^2 c^2} + \frac{2 \omega_{pe}^2}{k^2 c^2} \phi_6 \right],$$

$$D_4 = \frac{k_{\parallel} \omega}{k^2 c} \left\{ \frac{v_e}{c} \phi_2 \phi_5 - \frac{k^2 c v_e}{2 \omega_{pe}^2} \phi_4 \left[1 - \frac{\omega^2}{k^2 c^2} + \frac{2 \omega_{pe}^2}{k^2 c^2} \phi_1 \right] \right\},$$

$$D_5 = \left[1 - \frac{\omega^2}{k^2 c^2} + \frac{2 \omega_{pe}^2}{k^2 c^2} \phi_6 \right] \left[1 - \frac{\omega^2}{k^2 c^2} + \frac{2 \omega_{pe}^2}{k^2 c^2} \phi_1 \right], \quad D_6 = -\frac{4\omega_{pe}^4}{k^4 c^4} \phi_5^2.$$

$$\phi_1 = -\xi_e Z(\xi_e) \mu e^{-\mu} [I_0(\mu) - I_1(\mu)], \quad \phi_2 = -(2\mu)^{-1/2} \phi_1,$$

$$\phi_3 = -\xi_e Z(\xi_e) e^{-\mu} I_0(\mu), \quad \phi_4 = \frac{1 + \xi_e Z(\xi_e)}{Z(\xi_e)} \phi_3,$$

$$\phi_5 = \frac{1 + \xi_e Z(\xi_e)}{Z(\xi_e)} \phi_2, \quad \phi_6 = \xi_e \phi_4, \quad (A7)$$

$$\xi_i = (\omega - k_y v_o)/k v_i, \quad \xi_e = \frac{\omega}{k_{\parallel} v_e}, \quad \mu \approx k_y^2 v_e^2 / 2 \Omega_e^2, \quad (A8)$$

$$Z(\xi) = \pi^{-1/2} \int_{-\infty}^{\infty} dx \exp(-x^2)/(x-\xi). \quad (\text{A9})$$

and $I_n(\mu)$ being the modified Bessel function of order n . The dispersion equation is similar to that given in Eq. (16) of Wu et al. [1983].

ACKNOWLEDGMENT

This work was supported in part by NASA Grant NAG 5-759 to the Johns Hopkins University, Applied Physics Laboratory and in part by NASA Solar Terrestrial Theory Grant NAGW-971 to the University of Maryland.

FIGURE CAPTIONS

Figure 1 A schematic diagram to illustrate the suggestion that both the KCSI (operating in the neutral sheet) and the LHDI (operating outside the neutral sheet) play important roles in triggering substorms.

Figure 2a Wave frequency and growth rate maximized over wavenumber and propagation angle as a function of the relative drift speed.

Figure 2b The ratio of electromagnetic to electrostatic components of the excited waves for the KCSI.

Figure 3 Wave frequency and growth rate, maximized over the wavenumber, as a function of the propagation angle for $v_o/v_A = 15$.

REFERENCES

- Akasofu, S.-I., *Physics of Magnetospheric Substorms*, D. Reidel Publ. Co., Dordrecht, Holland, 1977.
- Baumjohann, W., Some recent progress in substorm studies, J. Geomag. Geoelectr., 38, 633-651, 1986.
- Cattell, C. A. and F. S. Mozer, Substorm-associated lower hybrid waves in the plasma sheet observed by ISEE-1, in Magnetotail Physics, ed. A. T. Y. Lui, Johns Hopkins University Press, Baltimore, p. 119-125, 1987.
- Chang, C.-L., H.-K. Wong, Kinetic instabilities driven by cross-field ion streaming motion, Trans. Amer. Geophys. Union, 70, 1270, 1989.
- Craven, J. D., and L. A. Frank, Diagnosis of auroral dynamics using global auroral imaging with emphasis on large-scale evolutions, in Auroral Physics, ed. by C.-I. Meng, Cambridge, England, 1989.
- Coroniti, F. V., Explosive tail reconnection: the growth and expansion phases of magnetospheric substorms, J. Geophys. Res., 90, 7427-7448, 1985.
- Galeev, A. A., Reconnection in the magnetotail, Space Sci. Rev., 23, 411-425, 1979.
- Huang, C. Y., C. K. Goertz, L. A. Frank, and G. Rostoker, Observational determination of the adiabatic index in the quiet time plasma sheet, Geophys. Res. Lett., 16, 563-566, 1989.
- Huba, J. D., N. T. Gladd, K. Papadopoulos, Lower hybrid drift wave turbulence in the distant magnetotail, J. Geophys. Res., 83, 5217-5226, 1978.

- Huba, J. D. and K. Papadopoulos, Non-linear stabilization of the lower hybrid drift instability by electron resonance broadening, Phys. Fluids, 21, 121-123, 1978.
- Huba, J. D., N. T. Gladd, and J. F. Drake, On the role of the lower hybrid drift instability in substorm dynamics, J. Geophys. Res., 86, 5881-5884, 1981.
- Kan, J. R., L. Zhu, S.-I. Akasofu, A theory of substorms: onset and subsidence, J. Geophys. Res., 93, 5624-5640, 1988.
- Kaufmann, R. L., Substorm currents: growth phase and onset, J. Geophys. Res., 92, 7471-7486, 1987.
- Lui, A. T. Y., Estimates of current changes in the geomagnetotail associated with a substorm, Geophys. Res. Lett., 5, 853-856, 1978.
- Lui, A. T. Y., J. R. Burrows, On the location of auroral arcs near substorm onsets, J. Geophys. Res., 83, 3342-3348, 1978.
- Lui, A. T. Y., R. E. Lopez, S. M. Krimigis, R. W. McEntire, L. J. Zanetti, and T. A. Potemra, A case study of magnetotail current sheet disruption and diversion, Geophys. Res. Lett., 15, 721-724, 1988.
- Rostoker, G., Triggering of expansive phase intensifications of magnetospheric substorms by northward turnings of the interplanetary magnetic field, J. Geophys. Res., 88, 6981-6993, 1983.
- Song, Y. and R. L. Lysak, Current dynamo effect of 3-D time-dependent reconnection in the dayside magnetopause, Geophys. Res. Lett., 16, 911-914, 1989.
- Speiser, T. W., Particle trajectories in model current sheets, 1. Analytical solutions, J. Geophys. Res., 70, 4219-4226, 1965.

- Winske, D., M. Tanaka, C. S. Wu, and K. B. Quest, Plasma heating at collisionless shocks due to the kinetic cross-field streaming instability, J. Geophys. Res., 90, 123-136, 1985.
- Wu, C. S., Y. M. Zhou, S. T. Tsai, S. C. Guo, D. Winske, and K. Papadopoulos, A kinetic cross-field streaming instability, Phys. Fluids, 26, 1259-1267, 1983.
- Wu, C. S., D. Winske, Y. M. Zhou, S. T. Tsai, P. Rodriguez, M. Tanaka, K. Papadopoulos, K. Akimoto, C. S. Lin, M. Leroy, and C. C. Goodrich, Microinstabilities associated with a high Mach number perpendicular bow shock, Space Sci. Rev., 37, 63-109, 1984.

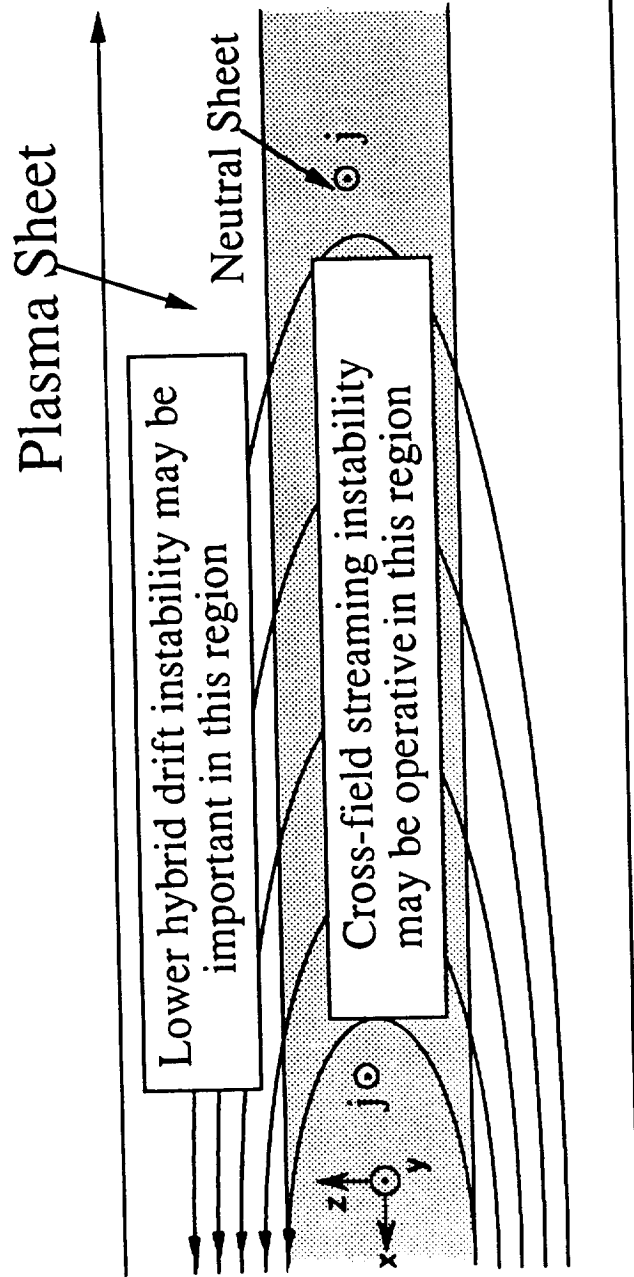


Figure 1

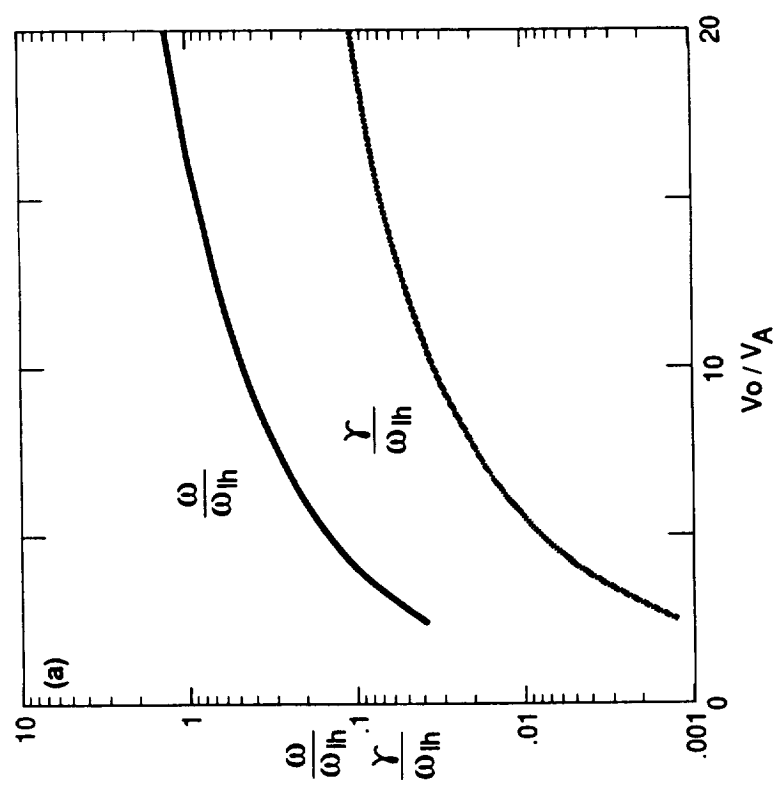
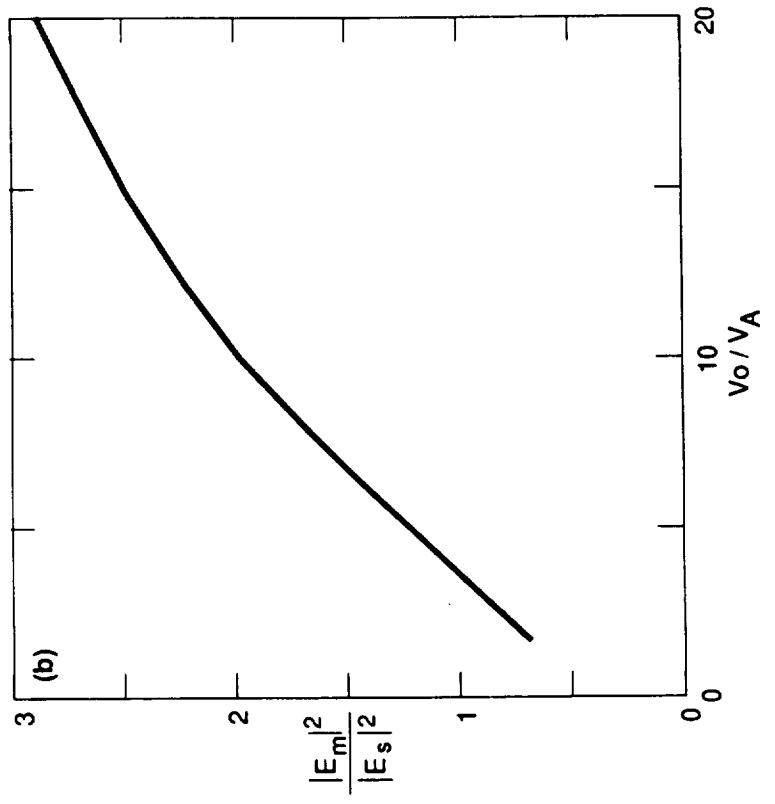


Figure 2

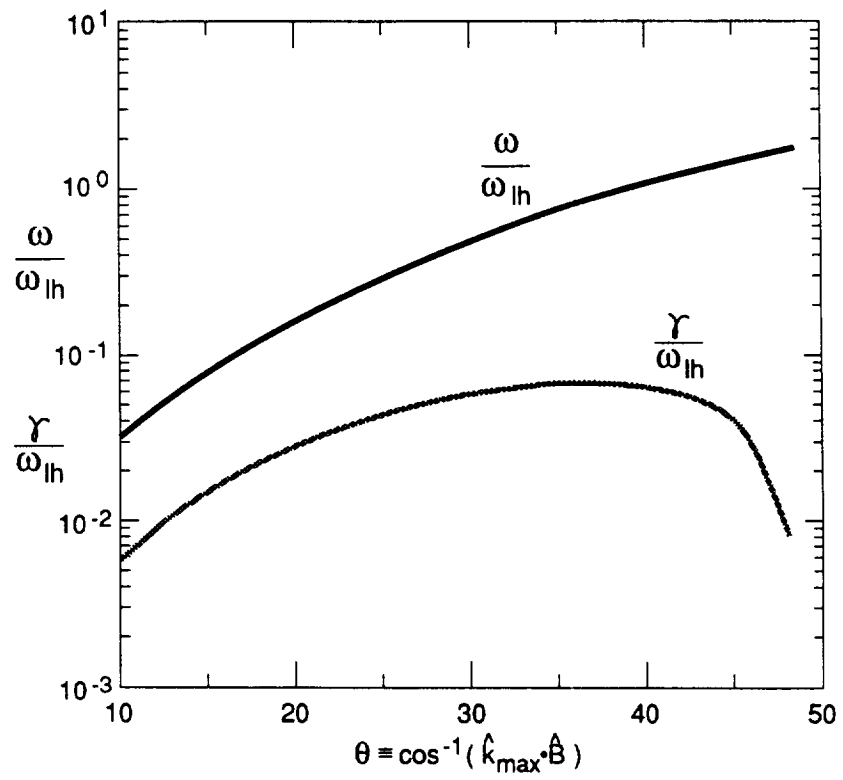


Figure 3